ORIGINAL ARTICLE

Anna Bergander · Jonas Brändström · Geoffrey Daniel
Lennart Salmén

Fibril angle variability in earlywood of Norway spruce using soft rot cavities and polarization confocal microscopy

Abstract The main purpose of this study was to investigate the variability of the fibril angle of tracheids in earlywood of Norway spruce (*Picea abies* L. Karst.). Polarization confocal microscopy was chosen and compared with the method utilizing the orientation of soft rot cavities. There was a significant correlation between the soft rot and polarization confocal microscopy methods, which showed the same trend of high fibril angles in the first part of the earlywood followed by a decrease toward the end of earlywood. This declining trend was less pronounced in annual rings containing compression wood. Moreover, large variations in fibril angle occurred between neighboring tracheids. The investigation also emphasized the differences between X-ray diffraction and microscopic methods, as the large variation seen by the latter methods is not seen by the X-ray diffraction approach because of its large area of measurement. No correlation was found between fiber morphology (i.e., average length, width, density) and the average fibril angle in the investigated annual rings.

Key words Fibril angle · *Picea abies* · Polarization confocal microscopy · Soft rot cavities · X-ray diffraction

Introduction

The S_2 layer of Norway spruce tracheids comprises about 80% of the cell wall,[1] and the properties of this layer

A. Bergander · L. Salmén
Swedish Pulp and Paper Research Institute (STFI), Stockholm, Sweden

J. Brändström (✉) · G. Daniel
Wood Ultrastructure Research Centre (WURC), Department of Wood Science, Swedish University of Agricultural Sciences, Box 7008, SE-750 07 Uppsala, Sweden
Tel. +46-18-67-26-07; Fax +46-18-67-34-89
e-mail: jonas.brandstrom@trv.slu.se

have an important effect on the behavior of spruce tracheids. One of the key structural features is the orientation of the cellulose fibrils, which have a helical orientation and high parallel order. The angle between the tracheid axis and the cellulose fibrils (i.e., the fibril angle) is known to have a major influence on the mechanical properties of wood[2-4] and pulp fibers[5-7] as well as on the shrinkage of wood.[8,9]

The average fibril angle varies in wood from the pith to the bark, being high close to the pith (i.e., juvenile wood) and decreasing toward the bark.[10-15] Within an annual ring the fibril angle of earlywood tracheids is known to be higher than that of latewood tracheids,[13,15-18] and the magnitude of the difference depends on the method used and the wood species investigated. Generally, X-ray diffraction,[13,19] where the average fibril angle is obtained from several tracheids, shows a small difference (1°–2°) between earlywood and latewood.[13,15,17,18] In contrast, microscopic methods (e.g., various methods using polarized light,[20-23] orientation of cross-field pit apertures,[11,24] directions of iodine crystals[25,26]) measure the local fibril angle within a tracheid and suggest larger differences (2°–30°) between earlywood and latewood.[16,18,24,27,28] This raises the question of the size and trends of variability among fibril angles of a population of tracheids in an annual ring.

During recent years techniques have been developed that enable detailed studies on the fibril angle of both wood and pulp fibers. For example, Kataoka et al.[29] used transmission electron microscopy (TEM) and Abe et al.[30,31] and Prodhan et al.[32] used field emission scanning electron microscopy (FE-SEM) to study microfibril deposition in differentiating tracheids. However, to study S_2 fibril angle variations in terms of tree growth conditions, more easily available techniques are needed. Such a technique is polarization confocal microscopy,[33,34] which involves optical sectioning of the cell wall and difluorescence (i.e., fluorescence depending on the direction of polarized illumination). In this case, difluorescence is obtained when the cell wall is stained using a fluorescent dye with a high affinity for cellulose fibrils. If polarization is parallel to the orientation of

the fibrils, maximum intensity occurs. Minimum intensity is obtained when polarization is perpendicular to the fibrils. Jang[34] found good agreement between polarizing confocal measurements and an earlier method of polarization microscopy of mercury-filled pulp fibers.[20] Another way to study the local orientation of cellulose fibrils is to measure the direction of cavities produced when soft rot fungi degrade fiber cell walls.[35-37] Anagnost et al.[36] found good agreement between X-ray diffraction, iodine staining, and orientation of soft rot cavities for the fibril angle of *Pinus taeda* L.

The purpose of the present work was to study the variability of fibril angles in annual rings of spruce wood. Earlywood tracheids were considered because they are predominant in the annual ring, and large variability of the fibril angle has been reported in this region.[38] The methods chosen were polarized confocal microscopy (for its ability to measure the local average fibril angle in individual cells) and soft rot fungi, a well-tested method for local fibril angle measurements. To determine if the variability in fibril angle continues into latewood, a small number of latewood tracheids were also investigated using polarization confocal microscopy. A comparison between the two microscopy methods and X-ray diffraction was conducted as well. In addition, the relation between fibril angle and fiber morphological features (e.g., fiber length, width, cell wall thickness) was investigated.

Materials and methods

Materials

Wood samples were obtained from an 18m high, 100-year-old Norway spruce tree (*Picea abies* L. Karst.) grown in mid-eastern Sweden. Disks 2cm thick were taken at 8m (40% of the total height), 1m, and ground level. From these disks, wood blocks containing the annual rings of interest (Table 1) were cut into 20 × 40 × 20mm blocks (W × B × H) and allowed to air-dry. Areas presumed to contain compression wood were selected based on the darker color of the surface area of newly cut disks. These areas may not in all cases be composed of fully developed compression wood.

Methods

Fibril angle by polarization confocal microscopy

Three radial wood sections from each annual ring, consisting of a single row of double radial walls, were obtained according to the method of Bergander and Salmén.[38] Sections were stained in a 0.1% aqueous solution of congo red for 40min at 60°–80°, rinsed thoroughly in water, and allowed to dry between a microscope slide and coverslip. All

Table 1. Average fibril angles (with 95% confidence intervals)

Annual ring (no.)	Wood type	Average fibril angle				X-ray diffraction (degrees)
		Soft rot cavities		Polarization CLSM		
		Degrees	95% CI	Degrees	95% CI	
8 m						
26	Normal	8	2	10	5	8
30	Normal	9	2	11	2	8
39	Normal	19	3	10	5	10
44	Compr.	19	1	26	4	29
61	Normal	7	2	9	2	7
61	Compr.	19	2	13	4	24
1 m						
12	Normal	14	4	14	6	8
36	Compr.	28	2	22	3	25
44	Normal	14	3	17	3	9
46	Normal	11	3	16	5	8
76	Compr.	16	3	15	6	9
77	Compr.	15	1	27	6	10
78	Normal	8	2	13	3	8
92	Normal	20	2	15	7	10
0.1 m						
37	Normal	19	3	24	7	23
38	Compr.	37	3	28	4	28
44	Normal	16	2	16	3	8
56	Normal	30	3	32	6	9
76	Normal	11	3	10	3	10

The results are based on about 30 randomly sampled earlywood tracheids using soft rot cavities and polarization confocal laser scanning microscopy (CLSM) as well as the average fibril angle at 50% ring width using X-ray diffraction at various heights on the tree. The standard deviation for the X-ray measurements was ±2°
CI, confidence interval; compr., compression

dry sections were then mounted on microscope slides in immersion oil and kept in darkness until measured using confocal laser scanning microscopy (CLSM).

The fibril angles were measured using a confocal scanning unit (BioRad Radiance 2000) equipped with a light microscope (Nikon Eclipse E800) and argon laser at an excitation at 488 nm. During measurements, a PLAN APO oil immersion ×60 objective with a depth resolution of 0.9 μm was used. To rotate the angle of incident polarization, a half-wave plate with rotating possibilities was inserted between the scan head and the specimen. Turning the half-wave plate by 5° caused a 10° turn of the passing linear laser beam. An image was acquired at each 10° over an interval of 180°. The pixel intensity of the difluorescence in these images was analyzed by the image analysis software Optimas 6.0 from Media Cybernetics and plotted against the angle of incident polarization. To determine the fibril angle accurately, plotted values were adjusted to Eq. (1).[34]

$$I = A \cdot \cos^2(P - \theta) + I_{min} \tag{1}$$

where I is the difluorescence pixel intensity, A is the amplitude of the curve, P is the angle of incident polarization, θ is the fibril angle, and I_{min} is the minimum difluorescence pixel intensity.

The S_2 layer of tracheids was localized by first focusing the laser beam on the upper S_3 layer, from the lumen side, of the double radial wall. The focal plane was then lowered 0.5 μm into the S_2 layer from where three successive measurements were recorded in the S_2 layer, each 0.3 μm lower than the preceding reading. The mean fibril angle of each tracheid was then recorded as the average of the three measurements. The standard deviation in fibril angle between measurements for these three levels in the z-direction was in the order of ±0.5°–2°, as shown in Fig. 1. Occasionally, the variation was as large as 10°, but such large variation was mostly related to an effect of tilted cell walls in the specimen, which was avoided wherever possible.
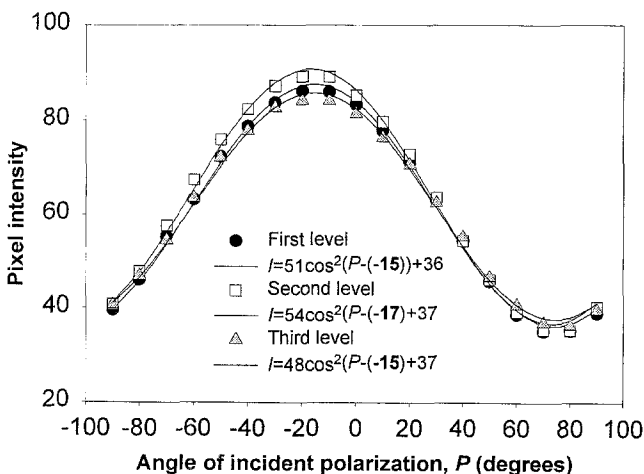
Fig. 1. Intensity curves for the same tracheid at three depths 0.3 μm apart within the S_2 layer. The **boldface characters** in the equations indicate the fibril angle. Standard deviation of the fibril angle for this particular tracheid was 1°

To measure earlywood tracheids exclusively, only the first 50% of the annual ring width was considered. Ten earlywood tracheids were randomly sampled from each section by assuming that each earlywood tracheid has a radial width of 30 μm. Fibril angle measurements were performed on three radial sections per annual ring, making a total of 30 earlywood tracheids per annual ring. The last-formed latewood tracheids were also examined from sections of three annual rings.

Fibril angle by orientation of soft rot cavities

A monoculture decay experiment was conducted to introduce soft rot cavities into the spruce wood without interference from other fungi. Glass jars were filled with moist compost and sterilized in an autoclave for 60 min at 120°C. Wood samples were then placed in the soil. Thereafter, the jars were resterilized for 30 min, as above. After cooling, the samples were inoculated with 5 ml of a mycelial suspension of the soft rot fungus *Phialophora mutabilis* (van Beyma) Schol-Schwarz. The jars were stored at 26°C and 80% relative humidity (RH) for 6 months.

When uniform soft rot attack had been obtained in the earlywood, three radial sections 20 μm thick were cut from each annual ring using a sledge microtome. Sections were mounted on microscope slides in aqueous 1% safranin, washed with glycerol, and observed using a Leica DMLS microscope. Digital images were acquired using a CCD camera and the image analysis software Image Pro Plus 4.0 from Media Cybernetics. Three soft rot cavities per tracheid were subjectively chosen and manually measured using the same software by first drawing a reference line parallel to the tracheid axis and then a line along the longitudinal axis of the soft rot cavity. Cavities equidistant from the tangential walls and in zones lacking pits were chosen. The standard deviation of cavity orientation in a tracheid usually varied between ±1° and ±5° (Fig. 2) when areas without distinctly different orientations were considered. Because of the variation in cavity orientation and the subjective choice of cavities, two persons measuring the same wood section occasionally rendered an error of approximately 10%.

Tracheids were selected in the same manner as for the polarization CLSM. To correlate and enable measurement of both polarization CLSM and soft rot cavities on the same cell walls, radial wood sections were also cut (according to the method of Bergander and Salmén[38]) from two soft rot decayed wood blocks. In this case, the orientation of soft rot cavities were determined using CLSM images instead of images from the light microscope.

Fibril angle measured by X-ray diffraction

The average fibril angle in the middle of each annual ring was determined by X-ray diffraction according to a method described by Sahlberg et al.[13] This method measures the intensity from the (040) plane in reflection. The measured area was 5.0 × 0.4 mm in the tangential and radial directions, respectively. The average angle (θ) was determined as

Fig. 2a–d. Soft rot cavities in tracheids viewed from the lumen side visualized by congo red and confocal laser scanning microscopy. **a** First-formed earlywood: average soft rot cavity orientation to the tracheid axis is 14° ± 2°. **b** End of earlywood: soft rot cavities are almost parallel to tracheid axis (1° ± 0.5°). **c** Compression wood, first-formed earlywood: average soft rot cavity orientation to the tracheid axis is 32° ± 3°. **d** Compression wood, end-of-earlywood tracheid: average soft rot cavity orientation to tracheid axis is 21° ± 1°. Bars 15 μm
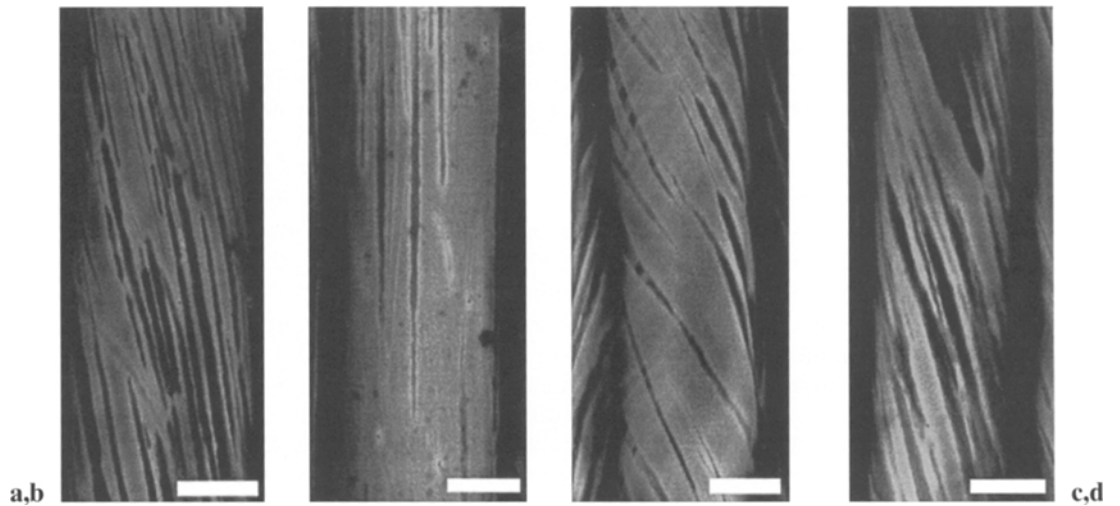
Table 2. Regression model for correlation between polarization confocal microscopy (dependent in this model) and orientation of soft rot cavities (predictor)

Model	Predictor	Coeff	SD	t	P
Measurements on identical cell walls of normal wood (R^2 81.4%)	Constant	2.74	1.62	1.69	0.105
	Soft rot	0.93	0.1	9.6	<0.0005
Measurements on identical cell walls of compression wood (R^2 36.9%)	Constant	3.95	6.36	0.62	0.54
	Soft rot	0.94	0.24	3.97	<0.0005
Average fibril angle of annual rings (R^2 58.4%)	Constant	6.20	2.51	2.47	0.02
	Soft rot	0.66	0.14	4.88	<0.0005

$\theta = 0.6T$ according to Cave[19] and Meylan.[39] One measurement was taken in the middle of each ring of the wood blocks later used for local fibril angle measurements by the two microscopic methods.

Wood and fiber characterization

Average fiber length and width were obtained by measurements using STFI FiberMaster[40] on chlorite-delignified wood from the entire annual ring (i.e., latewood fibers were included in the analysis). Cell wall thickness was approximated by the average density of earlywood obtained by X-ray microdensitometry.[41]

Results and discussion

Correlation between methods

There were no significant differences at the 95% level in a t-test between the soft rot and polarization confocal methods for the average fibrillar values from different positions in the tree or the individual fibrillar angle measurements. This was confirmed in a linear regression analysis, as seen by the low P value (Table 2). Figure 3 shows the relation between polarization CLSM and soft rot cavities when identical
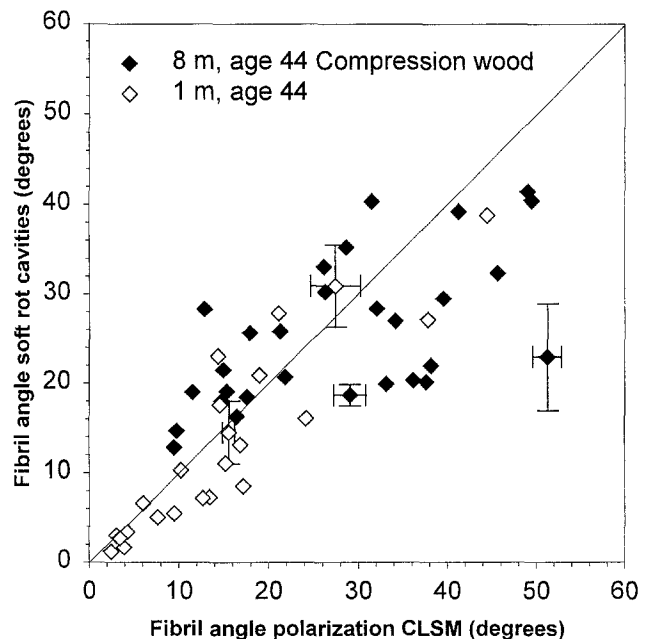
Fig. 3. Relation between fibril angle using polarization confocal laser scanning microscopy (CLSM) and soft cavities for the same area of the tracheid of earlywood tracheids from two annual rings. Earlywood tracheids from compression wood generally have higher fibril angles. The highest fibril angles for the annual ring without compression wood originate from the first earlywood tracheids in the annual ring. Standard deviation is indicated for four representative samples ($n = 3$)

areas of tracheid cell walls were measured. There was a tendency for the soft rot method to indicate slightly lower fibril angles than that indicated by polarization CLSM, especially for the annual ring containing compression wood (i.e., for fibril angles above 25°). For compression wood the reverse is usually true; that is, higher fibril angles are indicated by soft rot cavities than by polarized CSLM for compression wood (Table 1; see Fig. 5 later). For compression wood the fibril angle was difficult to measure using the soft rot method because the lignin content in these tracheids is higher. Soft rot fungi tend to avoid areas with a high lignin content,[42] and the number of cavities in these tracheids was consequently low. In tracheids toward the end of the early-wood area (Fig. 2b), cavities with an orientation of about 2° were often measured, whereas polarization CLSM in the same area consistently measured a fibril angle of >2°.

Fibril angle variation in earlywood

Figures 4 and 5 show the fibril angle variation in earlywood from four annual rings using polarization CLSM and soft rot cavities on separate sections (i.e., not the same tracheids but those from a nearby area in the same annual ring). Annual rings without compression wood showed a clear trend toward a higher fibril angle at the beginning of the earlywood region (Figs. 2, 4a) followed by a decrease toward the end of earlywood. The fibril angle ranged from a mean of 30° in the first earlywood tracheids to approximately 5° close to the end of earlywood. These results support the results of an earlier study by Herman et al.[28] that used the orientation of cross-field pit apertures to monitor the fibril angle at evenly spaced sites from earlywood to latewood. However, these authors found a linear relation between the fibril angle and the position in the annual ring, whereas this study showed a more scattered behavior of the fibril angle in earlywood. Although in the present study mostly earlywood tracheids were measured, it seems reasonable that the low fibril angle toward the end of the earlywood continues into the latewood. This was confirmed by measurements of the last-formed latewood tracheids in one annual ring without compression wood using polarization CLSM (Fig. 4b). From a physiological point of view, latewood is optimized to support the tree trunk with its thick cell walls and small lumens. A small fibril angle is also favorable in this respect. A recent study[43] using a new technique called "small-angle X-ray scattering" reports much higher fibril angles in the latewood (mean fibril angle 20°) than in the earlywood (mean fibril angle 0°) of Norway spruce. There was, no evidence of such findings based on the measurements reported here.

When discussing the fibril angle variation within a tree, it is important to remember the large variation that exists in annual rings. The results of this investigation showed that the fibril angle may be approximately six times higher at the beginning of earlywood than at the end, adjacent to the latewood. The method of measuring the fibril angle is clearly important when determining variation of fibril angle within annual rings.

a)

b)
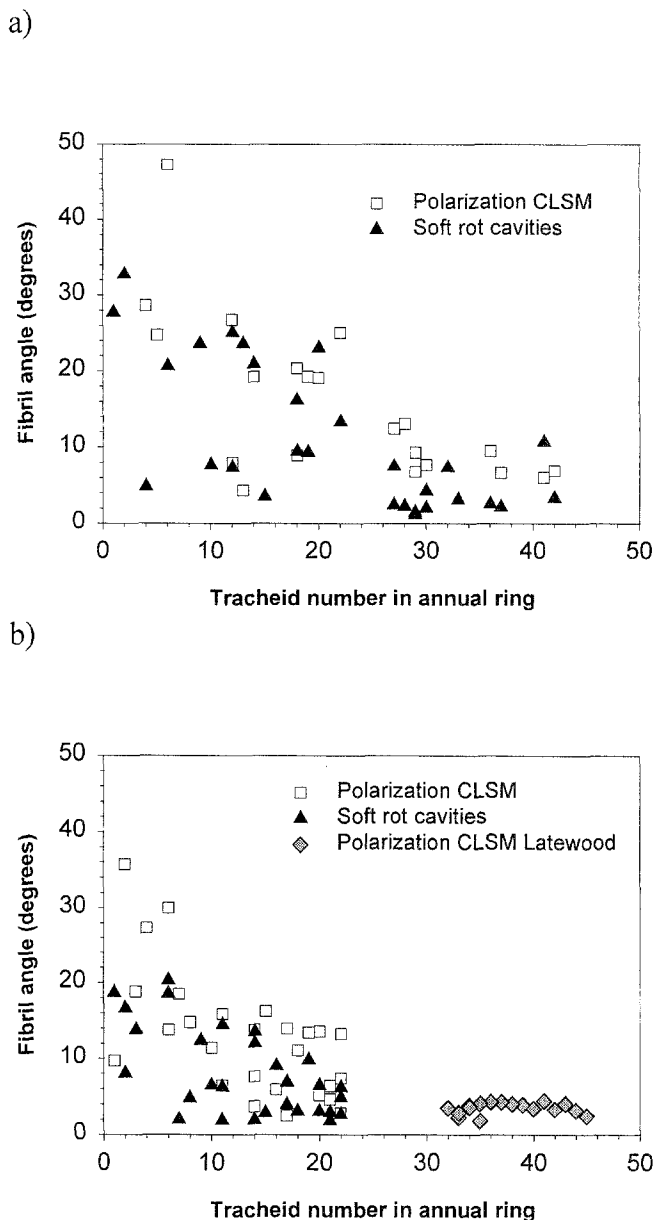
Fig. 4a,b. Fibril angle as a function of tracheid number. **a** Annual ring 46 at 1 m. **b** Annual ring 78 at 1 m height. Tracheid number 1 is the first earlywood tracheid in the annual ring. The fibril angle of the last-formed latewood tracheids was also measured by polarization CLSM in annual ring 78. Because of the random selection of sampling sites in each of the three wood sections examined for each annual ring and method, several measurements can be displayed for the same tracheid number

The mean fibril angle in earlywood was higher (i.e., about 30°) in annual rings containing compression wood than for tracheids from normal wood, and no decreasing trend toward latewood was observed (Fig. 5). The variation among neighboring tracheids was generally large. The fibril angle of the last-formed latewood tracheids was also determined for two of the annual rings containing compression wood (Fig. 5). These tracheids showed a higher, more scattered fibril angle than did tracheids in latewood lacking compression wood. In Fig. 5b, large variations in fibril angle

a)

b)
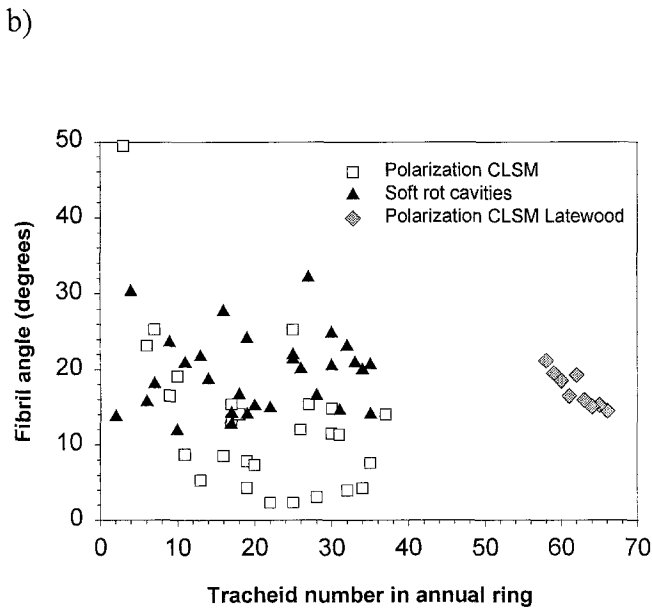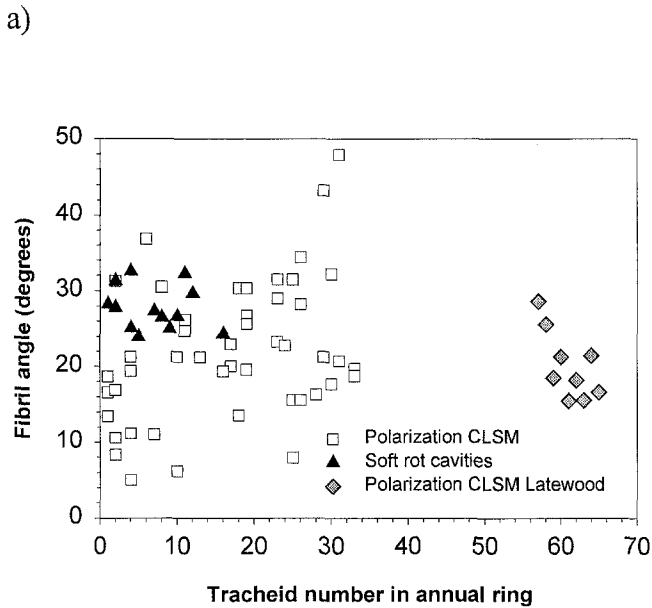
Fig. 5a,b. Mean fibril angle as a function of tracheid number. **a** Annual ring 36 at 1 m height. **b** Annual ring 61 at 8 m. Tracheid number 1 is the first earlywood tracheid in the annual ring. Both annual rings contain compression wood. Because soft rot avoids compression wood, there are fewer data points for this method. The fibril angle of the last-formed latewood tracheids was measured with polarization CLSM. Because of the random selection of sampling sites within each of the three wood sections examined for each annual ring and method, several measurements can be displayed for the same tracheid number

(i.e., 3°–30°) in earlywood were observed with polarization CLSM, whereas the fibril angle of latewood was around 18°. Variations in behavior of annual rings containing compression wood may serve as an explanation for the earlier mentioned reversed behavior for the fibril angle between earlywood and latewood reported by Lichtenegger et al.[43]
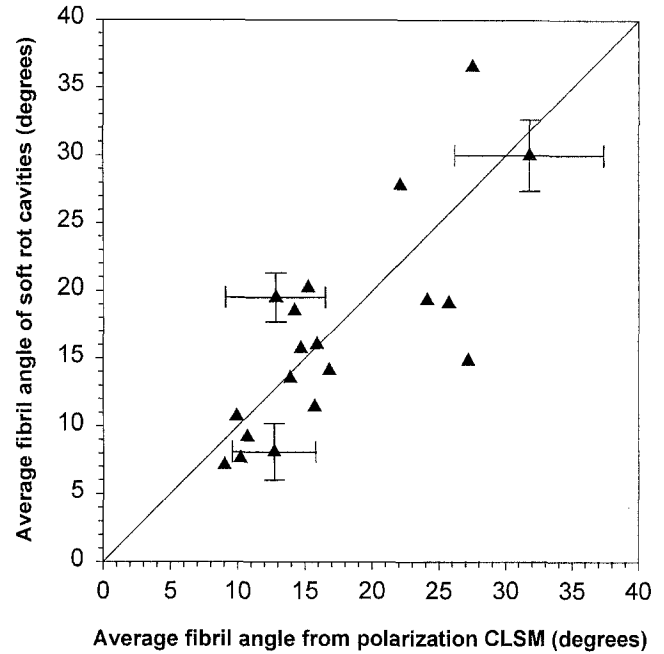
Fig. 6. Correlation between the average fibril angle of earlywood in annual rings determined by soft rot cavities and polarization CLSM. The 95% confidence interval is indicated for three representative annual rings

Average fibril angles

The average fibril angle for each of the annual rings is given in Table 1. The confidence intervals for the average fibril angle of each annual ring were large owing to the decreasing trend in fibril angle within the earlywood. Figure 6 shows that there was rather good correlation between the soft rot and polarization CLSM methods using the average fibril angle of each measured annual ring.

Results of X-ray diffraction measurements in the middle of each annual ring varied to a much lesser extent between annual rings than did results from the two microscopic methods (Table 1). Only annual rings containing compression wood had significantly higher fibril angles than those seen with the microscopic methods. The small variation between annual rings using X-ray diffraction made correlation between this method and the soft rot cavity and polarization CLSM methods indecisive (Fig. 7). Because X-ray diffraction measurements were performed at the center of each annual ring, and the microscopic measurements were carried out on the first half of the earlywood, the former method did not include the first tracheids in the ring where high fibril angles are found. Because of the decreasing trend in fibril angle in the earlywood region, these comparisons are thus inconclusive. By using only the average of fibril angle measurements from tracheids within the last 0.2 mm of the 50% earlywood region for the soft rot and polarization CLSM methods, corresponding to half of the radial distance with X-ray diffraction, a more appropriate comparison with the X-ray data was obtained. As can be seen in Fig. 7, comparing average values from the same position in annual rings reduced some of the discrepancy between the

a)

b)

Average fibril angle from X-ray diffraction (degrees)
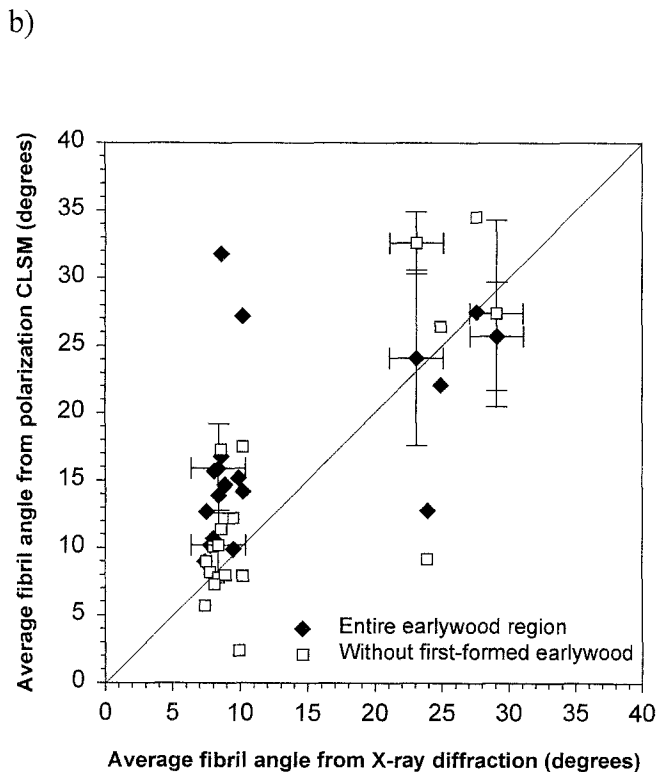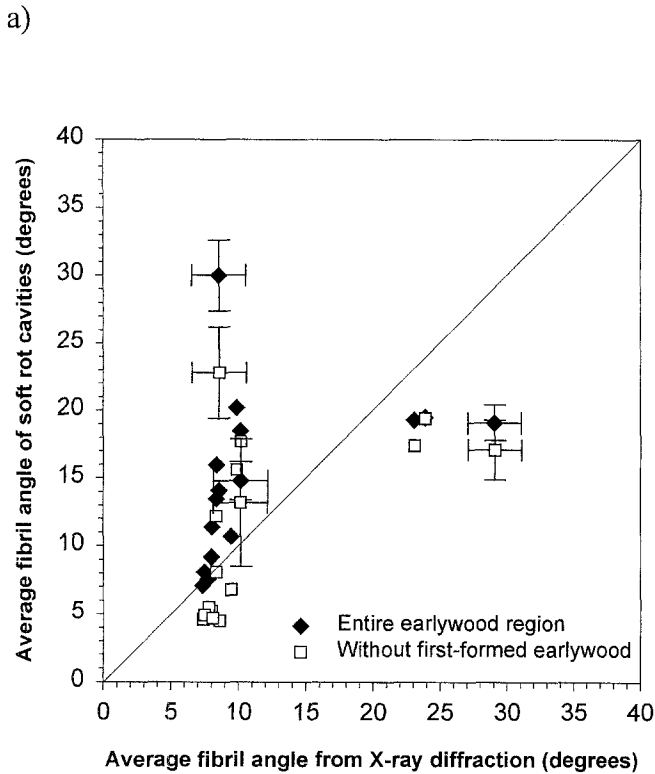
Fig. 7. Correlation between fibril angle measurements using X-ray diffraction and soft rot cavities (a) and polarization CLSM (b). The 95% confidence interval for the microscopic methods and the standard deviation for X-ray diffraction are indicated for three representative annual rings. Because of difficulties when measuring soft rot cavities in compression wood tracheids, four annual rings from Table 1 have been left out in a

methods. However, for annual rings with moderate fibril angles (i.e., <25°), the correlation was still not satisfactory. One possible reason for this deviation is the manner in which the measurements were conducted. Whereas the two microscopic methods focus on small, well-defined areas of tracheids, results of the X-ray diffraction measurements were obtained from much larger areas, including whole tracheids as well as ray tracheids and ray parenchymal cells. Differences in the measurement area may also explain the higher average fibril angles reported earlier[38] by X-ray diffraction compared to polarized CLSM, where the entire annual ring, including the low fibril angles of latewood, was measured. An earlier investigation[36] comparing the soft rot method with X-ray diffraction (002 plane) in loblolly pine (*Pinus taeda* L.) obtained an excellent correlation between the two methods ($R^2 = 0.94$). One reason for the reported agreement in that investigation may be that no cavities were present within the first-formed earlywood tracheids, or those tracheids were removed when earlywood and latewood was separated for soft rot degradation. However, a larger variation in fibril angle was noted in earlywood. Another reason may relate to the obtained higher fibril angles for loblolly pine compared with Norway spruce. At higher fibril angles, the present investigation also indicated a smaller discrepancy between the two methods.

Fiber morphology and fibril angle

No obvious correlation was found between fiber width or length (Table 3) and the average fibril angle (Table 1) in the annual rings. For example, the correlations were $R^2 = 0$ and 0.3, respectively, when the fiber length was correlated with the average fibril angle from polarization CLSM and soft rot cavity measurements. Although the average fiber width and length measurements in this study include latewood tracheids of the annual rings, the effect of the latewood cells on tracheid dimension should be relatively limited. Earlier studies suggesting that fiber length correlates with the fibril angle[44,45] are based on comparisons between properties of juvenile and mature wood; in other words, they are based on comparisons between fundamentally different tracheids. Preston[46] suggested that the angle of fibril deposition is related to the length of the tracheids. However, Hirakawa and Fujisawa[47] and Sahlberg et al.[13] did not find a clear correlation between fibril angle and tracheid length. In the present study, no correlation was found between average fibril angle and the average cell wall thickness from corresponding areas in the density profile ($R^2 = 0.2$). However, cell wall thickness determined in this way is not totally representative of the true cell wall thickness; it also depends on cell diameter, as discussed by Yasue et al.[48] Thus the correlation between cell wall thickness and fibril angle may have been concealed in this study.

Because the variation in morphology (including fiber width) and fibril angle is large in an annual ring, the relation between these parameters is lost in average measurements that examine the entire annual ring. For example, there are decreasing trends in both the fibril angle and the tracheid

Table 3. Average fiber dimensions obtained for each annual ring studied at various heights on the tree

Annual ring no.	Wood type	Average length ±3% (mm)	Average width ±3% (μm)	Average density (kg/dm³)
8 m				
26	Normal	3.0	40	0.27
30	Normal	3.2	37	0.28
39	Normal	3.4	37	0.26
44	Compr.	3.5	41	0.28
61	Normal	3.3	38	0.30
61	Compr.	3.1	34	0.33
1 m				
12	Normal	1.8	31	0.35
36	Compr.	2.8	39	0.38
44	Normal	2.9	35	0.30
46	Normal	2.7	38	0.34
76	Compr.	2.9	39	0.36
77	Compr.	2.9	39	0.38
78	Normal	3.1	37	0.31
92	Normal	3.0	38	0.29
0 m				
37	Normal	2.3	39	0.33
38	Compr.	2.1	40	0.35
44	Normal	2.6	37	0.30
56	Normal	2.5	38	0.34
76	Normal	2.5	39	0.32

Average length and width are length-weighted. The average density of the annual ring was obtained from microdensitometry measurements within the first 50% of the width of each annual ring

diameter[49] from earlywood to latewood, and a relation between these two parameters can be determined only if the properties of the same tracheid are compared.

Conclusions

The present study shows a significant correlation between measurements of the fibril angle by orientation of soft rot cavities and polarization CLSM methods in annual rings of Norway spruce. The two methods showed the same trend, with high fibril angles in the first part of the earlywood followed by a decrease in fibril angle toward the end of earlywood. There were also indications that large variations in fibril angle exist among neighboring cells, especially in annual rings containing compression wood. There was no correlation between fiber morphology (i.e., average length, width, density) and mean fibril angle. Because of the large variability in fibril angle in earlywood, average methods such as X-ray diffraction may not adequately reveal the true behavior of the tracheid population from annual rings.

References

1. Fengel D, Stoll M (1973) Variation in cell cross-sectional area, cell-wall thickness and wall layers of spruce tracheids within an annual ring. Holzforschung 27:1–7
2. Preston RD (1974) The physical biology of plant cell walls. Chapman and Hall, London, p 491
3. Cave ID (1969) The longitudinal Young's modulus of *Pinus radiata*. Wood Sci Technol 3:40–48
4. Bendtsen BA, Senft J, Senft JF (1986) Mechanical and anatomical properties in individual growth rings of plantation-grown eastern cottonwood and loblolly pine. Wood Fiber Sci 18:23–38
5. Page DH, El Hosseiny F, Winkler K, Lancaster APS (1977) Elastic modulus of single wood pulp fibers. TAPPI J 60:114–117
6. Armstrong JP, Kyanka GH, Thorpe JL (1977) S2 fibril angle-elastic modulus relationship of TMP Scotch pine fibers. Wood Fiber Sci 10:72–80
7. Kellogg RM, Thykesson E, Warren WG (1975) The influence of wood and fibre properties on kraft converting-paper quality. TAPPI J 58:113–116
8. Barrett JD, Schniewind AP, Taylor RL (1972) Theoretical shrinkage model for wood cell walls. Wood Fiber Sci 4:178–192
9. Meylan BA (1968) Cause of high longitudinal shrinkage in wood. For Prod J 18(4):75–78
10. Von Kollmann F, Antonoff M (1943) Beitrag zur Erforschung des submikroskopischen Feinbaus von Holz. Holz Roh Werkstoff 6:41–45
11. Hiller CH (1964) Correlation of fibril angle with wall thickness of tracheids in summerwood of slash and loblolly pine. TAPPI J 47:125–128
12. Donaldson LA (1992) Within- and between-tree variation in microfibril angle in *Pinus radiata*. NZ J For Sci 22:77–86
13. Sahlberg U, Salmén L, Oscarsson A (1997) The fibrillar orientation in the S2-layer of wood fibres as determined by X-ray diffraction analysis. Wood Sci Technol 31:77–86
14. Saranpää P, Serimaa R, Andersson S, Pesonen E, Suni T, Paakari T (1998) Variation of microfibril angle of Norway spruce (*Picea abies* (L.) Karst.) and Scots pine (*Pinus sylvestris* L.): comparing x-ray diffraction and optical methods. In: Butterfield BG (ed)

Microfibril angle in wood. University of Canterbury, Westport, NZ, pp 240–252

15. Marton R, Rushton P, Sacco JS, Sumiya K (1972) Dimensions and ultrastructure in growing fibers. TAPPI J 55:1499–1504

16. McMillin CW (1973) Fibril angle of loblolly pine wood as related to specific gravity, growth rate and distance from pith. Wood Sci Technol 7:251–255

17. Paakkari T, Serimaa R (1984) A study of the structure of wood cells by X-ray diffraction. Wood Sci Technol 18:79–85

18. Marton R, McGovern SD (1970) Relation of crystallite dimensions and fibrillar orientation to fiber properties. In: The physics and chemistry of wood pulp fibres. TAPPI 8:153–158

19. Cave ID (1966) Theory of X-ray measurement of microfibril angle in wood. For Prod J 16:37–42

20. Page DH (1969) A method for determining the fibrillar angle in wood tracheids. J Microsc 90:137–143

21. Leney L (1981) A technique for measuring fibril angle using polarized light. Wood Fiber Sci 13:13–16

22. Donaldson LA (1991) The use of pit apertures as windows to measure microfibril angle in chemical pulp fibers. Wood Fiber Sci 23:290–295

23. Ye C, Sundström O (1997) Determination of S2-fibril-angle and fiber-wall thickness by microscopic transmission ellipsometry. TAPPI J 80:181–190

24. Huang C, Kutcha NP, Leaf GL, Megraw RA (1998) Comparison of microfibril angle measurement techniques. In: Butterfield BG (ed) Microfibril angle in wood. University of Canterbury, Westport, NZ, pp 177–205

25. Bailey IW, Vestal MG (1937) The orientation of cellulose in the secondary wall of tracheary cells. J Arnold Arbor Harv Univ 18: 185–195

26. Senft JF, Bendtsen BA (1985) Measuring microfibrillar angles using light microscopy. Wood Fiber Sci 17:564–567

27. Kyrkjeeide PA (1990) A wood quality study of suppressed, intermediate and dominant trees of plantation grown *Picea abies*. Forest Products Laboratory, Madison, WI, p 145

28. Herman M, Dutilleul P, Avella-Shaw T (1999) Growth rate effects on intra-ring and inter-ring trajectories of microfibril angle in Norway spruce (*Picea abies*). IAWA J 20:3–21

29. Kataoka Y, Saiki H, Fujita M (1992) Arrangement and superimposition of cellulose microfibrils in the secondary walls of coniferous tracheids (in Japanese). Mokuzai Gakkaishi 38:327–335

30. Abe H, Ohtani J, Fukazawa K (1991) FE-SEM observations on the microfibrillar orientation in the secondary wall of tracheids. IAWA Bull 12:431–438

31. Abe H, Ohtani J, Fukazawa K (1992) Microfibrillar orientation of the innermost surface of conifer tracheid walls. IAWA J 13:411–417

32. Prodhan AKMA, Funada R, Ohtani J, Abe H, Fukazawa K (1995) Orientation of microfibrils and microtubules in developing tension-wood fibres of Japanese ash (*Fraxinus mandshurica* var. *Japonica*). Planta 196:577–585

33. Verbelen J-P, Stickens D (1995) In vivo determination of fibril orientation in plant cell walls with polarization CSLM. J Microsc 177(Pt 1):1–6

34. Jang HF (1998) Measurement of fibril angle in wood fibres with polarization confocal microscopy. J Pulp Pap Sci 24:224–230

35. Khalili S (1999) Microscopical studies on plant fibre structure. PhD thesis, Department of Wood Science, Swedish University of Agricultural Sciences, Uppsala, p 33

36. Anagnost SE, Mark RE, Hanna RB (2000) Utilization of soft-rot cavity orientation for the determination of microfibril angle. Part I. Wood Fiber Sci 32:81–87

37. Khalili S, Nilsson T, Daniel G (2001) The use of soft rot fungi for determining the microfibrillar orientation in the S2 layer of pine tracheids. Holz Roh Werkst 58:439–447

38. Bergander A, Salmén L (2000) Variations in transverse fibre wall properties: relations between elastic properties and structure. Holzforschung 54:654–660

39. Meylan BA (1967) Measurement of microfibril angle by X-ray diffraction. For Prod J 17(5):51–58

40. Karlsson H, Fransson P-I, Mohlin U-B (1999) STFI fibermaster. Proceedings of the 6th international conference on new available technologies. June 1–4, 1999, Stockholm, SPCI, Sweden, pp 367–374

41. Polge H (1978) Fifteen years of wood radiation microdensiometry. Wood Sci Technol 12:187–196

42. Nilsson T, Daniel G, Kirk TK, Obst JR (1989) Chemistry and microscopy of wood decay by some higher ascomycetes. Holzforschung 43:11–18

43. Lichtenegger H, Reiterer A, Stanzl TSE, Fratzl P (1999) Variation of cellulose microfibril angles in softwoods and hardwoods: a possible strategy of mechanical optimization. J Struct Biol 128:257–269

44. Kantola M, Seitsonen S (1969) On the relation between tracheid length and microfibrillar orientation measured by X-ray diffraction in conifer wood. Ann Acad Sci Fenn 300:2–10

45. Necesany V (1961) The variation of "normal" wood in view of its structure. Faserforsch Textiltechn 12:169–178

46. Preston RD (1934) The organization of the cell wall of the conifer tracheid. Philos Trans R Soc Lond Biol 224:131–173

47. Hirakawa Y, Fujisawa Y (1995) The relationships between microfibril angles of the S2 layer and latewood tracheid lengths in elite sugi tree (*Cryptomeria japonica*) clones (in Japanese). Mokuzai Gakkaishi 41:123–131

48. Yasue K, Funada R, Kobayashi O, Ohtani J (2000) The effects of tracheid dimensions on variations in maximum density of *Picea glehnii* and relationships to climatic factors. Trees Struct Function 14:223–229

49. Gindl W, Wimmer R (2000) Relationship between lignin content and tracheid morphology in spruce. In: Proceedings of 3rd plant biomechanics conference, August–September, Freiburg, Germany, pp 163–168